

## Electric field-controlled magnetization in exchange biased IrMn/Co/PZT multilayers

This content has been downloaded from IOPscience. Please scroll down to see the full text.

2013 Adv. Nat. Sci: Nanosci. Nanotechnol. 4 025017

(<http://iopscience.iop.org/2043-6262/4/2/025017>)

View [the table of contents for this issue](#), or go to the [journal homepage](#) for more

Download details:

IP Address: 103.234.89.167

This content was downloaded on 08/05/2016 at 08:44

Please note that [terms and conditions apply](#).

# Electric field-controlled magnetization in exchange biased IrMn/Co/PZT multilayers

D T Huong Giang<sup>1,2</sup>, N H Duc<sup>1</sup>, G Agnus<sup>2</sup>, T Maroutian<sup>2</sup> and P Lecoeur<sup>2</sup>

<sup>1</sup> Nano Magnetic Materials and Devices Department, Faculty of Engineering Physics and Nanotechnology, VNU University of Engineering and Technology, Vietnam National University, Hanoi, E3 Building, 144 Xuan Thuy Road, Cau Giay, Hanoi, Vietnam

<sup>2</sup> Institut d'Electronique Fondamentale, UMR CNRS and Université Paris-Sud, F-91405 Orsay, France

E-mail: [giangdh@vnu.edu.vn](mailto:giangdh@vnu.edu.vn)

Received 28 February 2013

Accepted for publication 3 April 2013

Published 8 May 2013

Online at [stacks.iop.org/ANSN/4/025017](http://stacks.iop.org/ANSN/4/025017)

## Abstract

Electric-field modulating exchange bias and near 180° deterministic magnetization switching at room temperature are demonstrated in simple antiferromagnetic/ferromagnetic/ferroelectric (AFM/FM/FE) exchange-coupled multiferroic multilayers of IrMn/Co/PZT. A rather large exchange bias field shift up to  $\Delta H_{\text{ex}}/H_{\text{ex}} = 500\%$  was obtained. This change governs mainly the electric-field strength rather than the applied current. It is explained as being realized through the competition between the electric-field induced uniaxial and unidirectional anisotropies. These results show good prospects for low-power spintronic devices.

**Keywords:** magnetoelectric coupling, exchange bias field, magnetization switching, piezoelectric, electric-field induced magnetization

**Classification numbers:** 4.11, 5.00

## 1. Introduction

Modern spintronics has become increasingly important because of its potential impact on memory technologies and magnetic sensors (see [1–5] and references therein). Traditionally, the function of these devices is based on the magnetic-field induced magnetization switching. In nanostructures, however, this physical mechanism is not efficient enough to control the magnetic bits due to the large current. In particular, when approaching the downscaling limits (e.g. in densely packed arrays) the unavoidable distribution of writing parameters coupled to the large stray fields will lead to spreading program errors and may cause influence on neighborhood architectures. In this context, the current-induced (or spin-transfer driven) switching mode is considered to be more efficient; however, two main facts still

remain challenging for applications in information storage technologies. Firstly, all metal spintronic devices have low resistances; secondly, the critical current density to move domain walls is still too high for the economization of the power consumption [2]. In order to tackle these difficulties, electric (E) field-induced magnetization switching is a prospective solution [1, 3–6]. That approach includes E-field induction of carrier density in semiconductor systems [7], high  $k$  electrolyte and insulator to change interfacial electronic states [8] and magnetoelectric effect, which occurs in multiferroic-type materials consisting of both ferromagnetic and ferroelectric orders [9–11].

For magnetoelectric coupling systems, the main principle of E-field controlled magnetization manipulation is that ferroelectric phases are used to generate strain that is transferred to the magnetic phase and the magnetization orientation can be influenced, thanks to the inverse magnetostriction (Villari effect) [12]. In this case, the stress sensing phase is preferred with a highly magnetostrictive material where the maximal change in the magnetization



Content from this work may be used under the terms of the [Creative Commons Attribution 3.0 licence](http://creativecommons.org/licenses/by/3.0/). Any further distribution of this work must maintain attribution to the author(s) and the title of the work, journal citation and DOI.

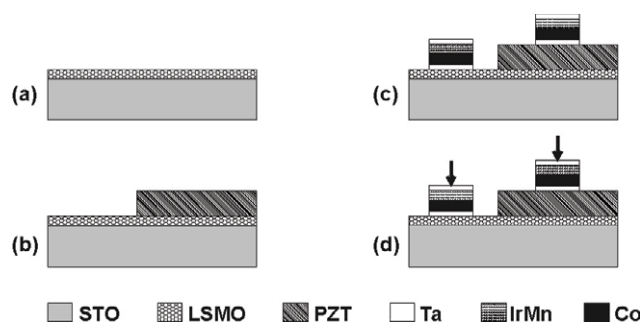


**Figure 1.** Schematic of microfabrication process for patterned Ta/IrMn/Co/Ta/PZT/LSMO/STO structures. (a) Bottom electrode LSMO layer grown on the STO(001) substrate; (b) the heterostructure of PZT layer was epitaxially deposited on a part of the top of LSMO layer using a mark to shield; (c) the magnetic structures Ta/Co/IrMn/Ta, which act as caps as well as electrode layers was deposited by sputtering technique via circular holes fabricated using UV lithography and liftoff; and (d) finally, mounting chip on a plastic printed board, electrically bottom and top contacted using wire bonding.

direction can reach up to  $90^\circ$ . This concept of the strain-driven magnetization rotation has been demonstrated in several spin-valve based multiferroic heterostructures, in which both the E-field induced magnetization and magnetoresistance were reported [13–16]. On the other hand, E-field control of exchange bias in antiferromagnetic/ferromagnetic/ferroelectric (AFM/FM/FE) heterostructures could lead to deterministic  $180^\circ$  magnetization switching. This is of great significance for information storage such as magnetoelectric random access memories (MERAM), but has still been difficult to realize [3, 17–19].

In this work we report an alternative approach in achieving power-efficient E-field control of exchange bias in high-quality AFM/FM/FE IrMn/Co/PZT multiferroic multilayers, where the near  $180^\circ$  deterministic-type magnetization switching is investigated using the inverse piezoelectric effect.

## 2. Experimental

Before fabricating  $\text{Pb}(\text{Zr}, \text{Ti})\text{O}_3$  (PZT) films, a 40 nm-thick  $\text{La}_{0.67}\text{Sr}_{0.33}\text{MnO}_3$  (LSMO) layer was firstly epitaxially grown on 500  $\mu\text{m}$ -thick  $\text{SrTiO}_3$  (STO)/Si(001) substrate by pulsed

laser deposition (PLD). The 220 nm-thick PZT films were then epitaxially grown at  $600^\circ\text{C}$  on the LSMO/STO substrate. In this case, a KrF excimer laser of 248 nm wavelength was used with 2 Hz repetition and about  $2.2 \text{ mJ cm}^{-2}$  energy density in an  $\text{O}_2$  gas pressure of 120 mTorr for LSMO deposition and in a  $\text{N}_2\text{O}$  ambient of 260 mTorr for PZT deposition, followed by a cooling-down procedure under 300 Torr of pure oxygen atmosphere. The exchange coupled to the strong AFM/FM IrMn/Co magnetic bilayer system is realized in the structure of Ta/Co/IrMn/Ta by magnetron sputtering with low Ar pressure of  $5.8 \times 10^{-4}$  mTorr at room temperature on top of the PZT layer. During the deposition, an external magnetic field of 1000 Oe was applied along [001] direction of single crystal PZT to induce an in-plane magnetic easy axis and exchange coupling. The patterned films are fabricated using micro-patterning techniques processes as illustrated in figure 1. In this configuration, Ta/Co/IrMn/Ta structures act as a cap as well as electrode layers.

The x-ray diffraction (XRD) system (Rigaku 3272) with Cu-K $\alpha$  radiation was used to examine the crystal orientation of the PZT films. The surface morphology of the PZT films was characterized by atomic force microscopy (AFM) measurements. A ferroelectric test system (Precision LC Radiant Technology) was used to measure their electrical properties. Two types of measurements were applied in this work: firstly, the bottom electrode Ta/Co/IrMn/Ta/LSMO is connected to the drive of the precision LC (denoted as the positive branch), and secondly, the Ta/Co/IrMn/Ta top electrode is connected to the drive (i.e. negative branch). Magnetic properties are investigated by means of the magneto-optical Kerr effect (MOKE). All experimental measurements are performed at room temperature.

## 3. Experimental results and discussion

A typical  $\theta$ - $2\theta$  XRD patterns spectrum of a 220 nm-thick PZT film grown on LSMO/STO/Si(001) is shown in figure 2(a), indicating a purely (00 $l$ ) orientated perovskite structure. It indicates that the LSMO and PZT layers are preferentially oriented along the  $c$ -axis perpendicular to the surface of STO substrate. The AFM images with scanning  $1 \times 1 \mu\text{m}^2$  area are shown in figure 2(b). The two-dimensional AFM picture manifests that most of the PZT grains are

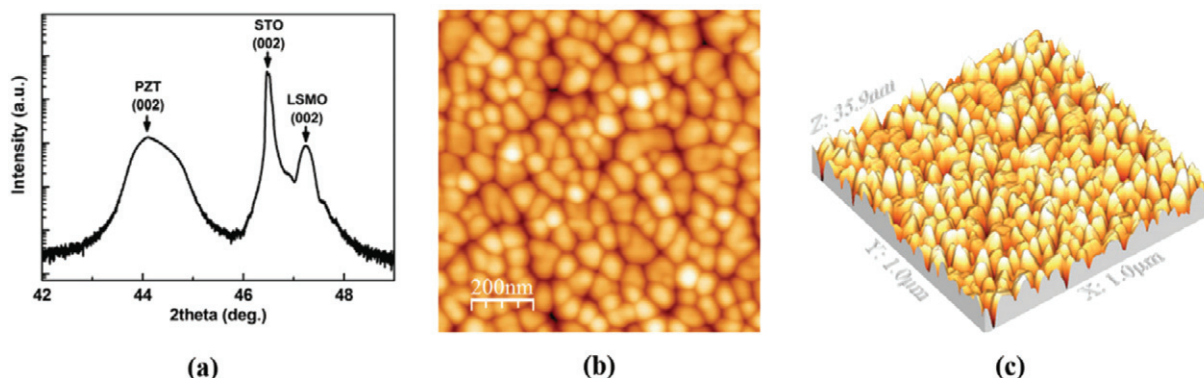


**Figure 2.**  $\theta$ - $2\theta$  XRD patterns of the as-deposited PZT/LSMO/STO thin film plotted in logarithmic scale. (a) 2D- and 3D-AFM image recorded over the scan area  $1 \times 1 \mu\text{m}^2$  (b) of the PZT thin films deposited on 40 nm-thick LSMO bottom electrode layer before micro fabricating.

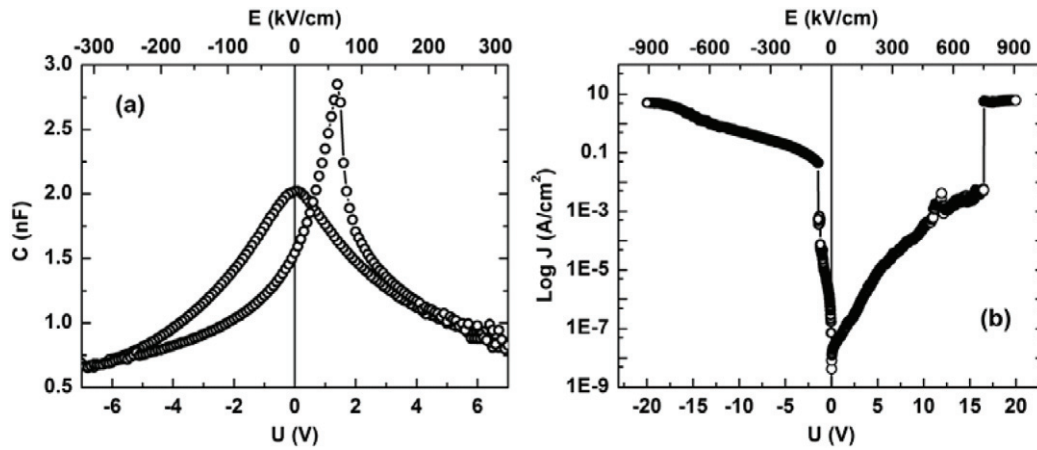


Figure 3.  $C-V$  (a) and  $J-V$  (b) characteristics of {Ta/IrMn/Co/Ta}/PZT/LSMO/STO film.

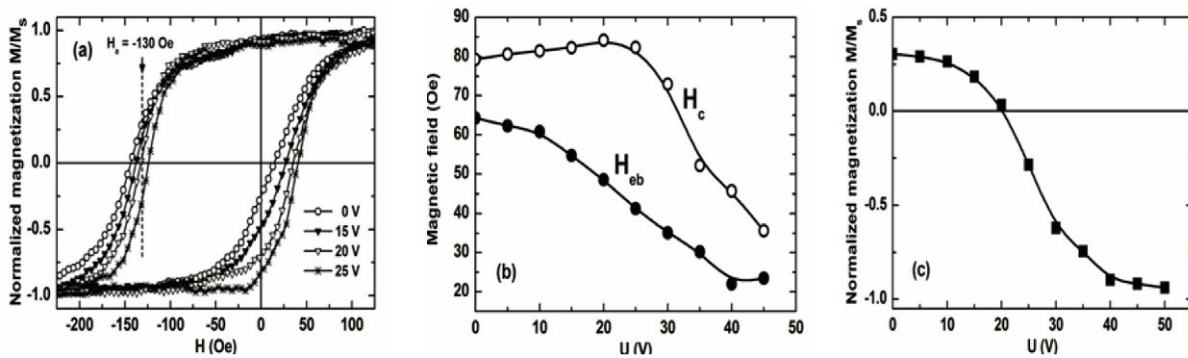


Figure 4. Magnetization loops measured under bias voltages  $V \leq 25$  V (a), magnetic coercivities and exchange bias fields (b) and magnetization change under applied voltage at the fixed magnetic field of  $-132$  Oe (c). The bias voltages are connected to the bottom electrode (positive branch).

equiaxed. The three-dimensional photograph, however, shows conical-shaped grains with a root-mean-square roughness of about 3 nm, which promotes a sufficiently flat surface for the subsequent growth of the magnetic layers (figure 2(c)).

Shown in figure 3(a) is the  $C-V$  (and the corresponding conventional  $C-E$ ) characteristics performed at 10 kHz for the investigated PZT films. The drive is connected to the bottom electrode (i.e. in the positive branch) and the dc voltage was swept from 7 to  $-7$  V and then reversely swept again. In this case, the  $C-V$  characteristic exhibits the typical butterfly shape with asymmetry. The coercivity is shifted to the positive applied voltage and an enhancement of the capacitance is accompanied. Indeed, the coercive fields of the film are of  $+63.6$  and  $-4.5$   $\text{kV cm}^{-1}$ , which yield an absolute coercive field of  $34.05$   $\text{kV cm}^{-1}$ . This asymmetry can be related to the dissimilar electrodes with different mobile and interface charge traps [20] and different work function [21].

Presented in figure 3(b) is the leakage current density data, indicating a more pronounced asymmetry. For the negative branch, the leakage current strongly increases at the low applied voltages (between 1.0 and 1.5 V), and reaches a value as large as  $10^{-1}$   $\text{A cm}^{-2}$  at  $E = 60$   $\text{kV cm}^{-1}$ . This large current density increases with increasing voltage and finally almost saturates with a value of  $10$   $\text{A cm}^{-2}$  at  $E > 875$   $\text{kV cm}^{-1}$ . For the positive branch, leakage currents as low as  $10^{-3}$   $\text{A cm}^{-2}$  remain in the electrical fields up to  $-800$   $\text{kV cm}^{-1}$ , indicating a high structural quality of the

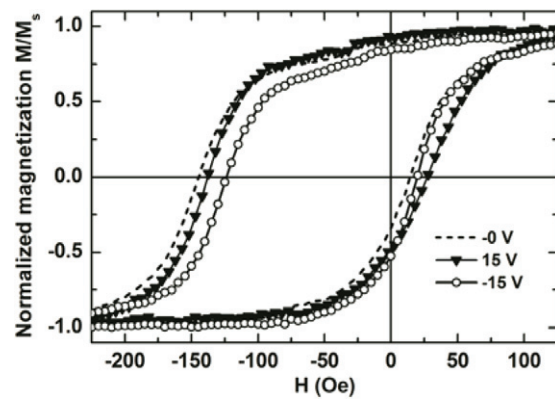
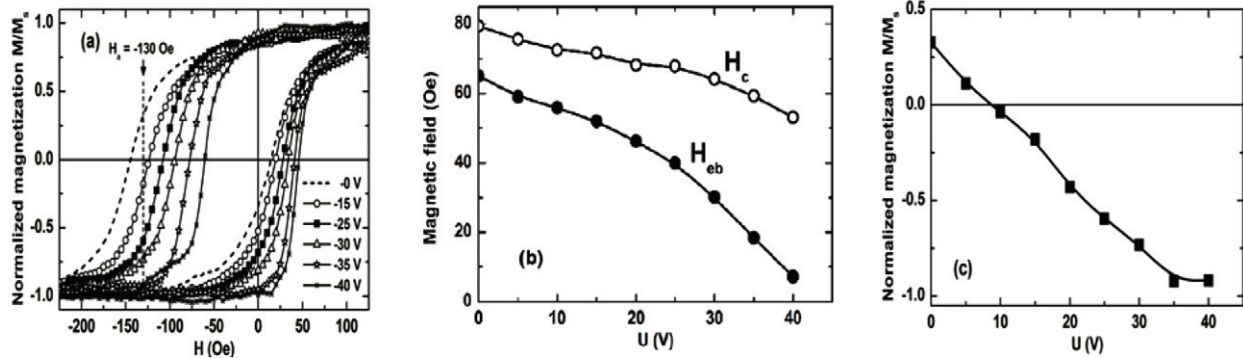


Figure 5. Magnetization loops measured under applied voltage for the positive (15 V) and negative ( $-15$  V).

ferroelectric layer. The leakage current jumps up at  $E = -810$   $\text{kV cm}^{-1}$  and the saturation follows after. Note that between  $+17$  and  $-17$  V applied voltage, the corresponding leakage current is always much higher for the negative branch than for the positive one, e.g.  $-5$  V;  $10^{-1}$   $\text{A cm}^{-2}$  and  $5$  V;  $10^{-5}$   $\text{A cm}^{-2}$ . This may relate to the fact that the Schottky barrier between magnetic and PZT layers induced a diode behavior [6, 22].

Large electrical currents flowing into the structure under electric field may give a certain contribution of the Joule effect and may affect the magnetic properties of the magnetic layers.



**Figure 6.** Normalized magnetization loops measured under bias voltages up to 40 V (a), magnetic coercivities and exchange bias fields (b) and magnetization change under applied voltage at the fixed magnetic field of  $-132$  Oe. The bias voltages are connected to the top electrode (negative branch).

In order to avoid this factor, the positive branch configuration was firstly considered, where the low leakage current almost exists in the whole applied voltage range. The normalized magnetization loops measured under various bias voltages (V) are illustrated in figure 4(a). It is clearly seen that, for the unbiased sample ( $V = 0$ ), the existence of a clear shift of the loop reflects the existence of an exchange bias field  $H_{ex}$  ( $\approx 79.5$  Oe). When applying a bias-voltage across the PZT layer, the negative magnetic coercivity decreases, while the positive field increases, indicating the suppression of  $H_{ex}$  (figure 4(b)). Inspection of the magnetic loops in figure 4(a) suggests that it should be possible to reverse the magnetization of the magnetic layer upon suitable electric and magnetic field biasing. A modification of the magnetization can be indeed processed in fixing an external magnetic field of  $H_a = -132$  Oe as shown by the arrow in figure 4(a). At this bias magnetic field, the normalized magnetization  $M/M_s$  already lowers to the value of 0.32 at  $V = 0$ . When increasing applied voltage  $V$ , the magnetization continues to lower, switches its sign at  $V \approx 20$  V and reaches the value of  $-0.32$  at about  $V \approx 25$  V. This electric-field bias dependence of the magnetization is described in figure 4(c). Electric-field tuning of exchange bias and deterministic magnetization reversal observed in AFM/FM/FE multilayers can be understood as an intrinsic magnetization phenomenon resulting from the competition between the effective uniaxial anisotropy  $K_{eff}$  (consists of the uniaxial anisotropy constant  $K_u$  and the E-field induced elastic anisotropy term of  $(3/2)\lambda\sigma$ ) and the anisotropy energy  $K_{ex}$  associated with the unidirectional exchange coupling [23, 24].

Although the leakage current exhibits the abrupt change between the applied voltage of 15 and 20 V, the variation of the magnetic coercivity and exchange bias field reflects almost a unique tendency for the whole applied voltage range (see figure 4(b)). This may imply that the magnetic change depends mainly on the amplitude of the electric field rather than the applied current. To tackle this point, the magnetic loops measured under the bias voltages of 15 V (with the current of 0.052 mA) and of  $-15$  V (with the current of 2.2 mA) are illustrated in figure 5. Surprisingly, although the current is 40 times larger for the latter case, the difference in coercivity field is a few per cent only. Thus, this encourages measurement of the magnetic loops under the bias voltage up to  $-40$  V to study the piezoelectric effect on the magnetization switching. The results are presented

in figure 6(a). It can be seen from this figure that when a voltage of 40 V is applied,  $H_{ex}$  significantly decreases from 60 to 10 Oe with  $\Delta H_{ex}/H_{ex}(40\text{ V}) = 500\%$ . As shown by the arrow in this figure, at the external bias magnetic field of  $-100$  Oe, the normalized magnetization  $M/M_s$  already lowers down to the value of 0.65. When increasing applied voltage  $V$ , the magnetization continues to lower, switches its sign between  $-25$  and  $-30$  V and finally reaches the value of  $-0.8$  at about  $V = -40$  V. The observed electric-field bias dependence of the magnetization is described in figure 6(b). Clearly, the near  $180^\circ$  deterministic magnetization switching can be electrically realized in the investigated AFM/FM/FE multiferroic multilayers.

#### 4. Conclusion

To summarize, high-quality piezoelectric films have been fabricated and used for electrically controlling the exchange bias in AFM/FM/FE IrMn/Co/PZT multiferroic multilayers. A rather large exchange bias field shift up to  $\Delta H_{ex}/H_{ex} = 500\%$  was obtained. The asymmetry is observed in both  $C-V$  and  $J-V$  characteristics, however, the exchange bias field change depends mainly on the electric-field strength rather than the applied current. The observed deterministic magnetization switching near  $180^\circ$  shows great potential in E-field writing of novel spintronics and memory devices.

#### Acknowledgment

This work was partly supported by the NAFOSTED of Vietnam under the project number 103.02.86.09.

#### References

- [1] Eerenstein W, Mathur N D and Scott J F 2006 *Nature* **442** 759
- [2] Maekawa S 2006 *Concepts in Spin Electronics* (Oxford: Oxford Science Publications)
- [3] Liu M, Lou J, Li S and Su N X 2011 *Adv. Funct. Mater.* **21** 2593
- [4] Scott J F 2007 *Nature Mater.* **6** 256
- [5] Bibes M and Barthelemy A 2008 *Nature Mater.* **7** 425
- [6] Lei N, Park S, Lecoer P, Ravelosona D, Chappert C, Stelmakhovych O and Holy V 2011 *Phys. Rev. B* **84** 012404
- [7] Chiba D et al 2008 *Nature* **455** 515
- [8] Endo M et al 2010 *Appl. Phys. Lett.* **96** 212503
- [9] Hu J M and Nan C W 2009 *Phys. Rev. B* **80** 224416

- [10] Allibe J *et al* 2010 *Appl. Phys. Lett.* **96** 142509
- [11] Lei N, Park S, Lecoeur P, Ravelosona D and Chappert C 2011 *Phys. Rev. B* **84** 012404
- [12] Mamin H J, Gurney B A, Wilhoit D R and Speriosu V S 1998 *Appl. Phys. Lett.* **72** 3220
- [13] Liu M *et al* 2009 *Adv. Funct. Mater.* **19** 1826
- [14] Lou J, Liu M, Reed D, Ren Y H and Sun N X 2009 *Adv. Mater.* **21** 4711
- [15] Chen Y, Fitchorov T, Vittoria C and Harris V G 2010 *Appl. Phys. Lett.* **97** 052502
- [16] Huong Giang D T, Thuc V N and Duc N H 2012 *J. Magn. Mater.* **324** 2019
- [17] Kleemann W 2009 *Physics* **2** 105
- [18] Catalan G and Scott J F 2009 *Adv. Mater.* **21** 2463
- [19] He X *et al* 2010 *Nature Mater.* **9** 579
- [20] Xiao B, Gu X, Izyumskaya N, Avrutin V, Xie J Q and Morkoc H 2007 *Appl. Phys. Lett.* **91** 182906
- [21] Masruroh and Toda M 2011 *Int. J. Appl. Phys. Math.* **1** 144
- [22] Khan M A, Comyn T P and Bell A J 2008 *Appl. Phys. Lett.* **92** 072908
- [23] Chung S H, Hoffmann A and Grimsditch M 2005 *Phys. Rev. B* **71** 214430
- [24] Camarero J, Sort J, Hoffmann A, Garcia-Martin J M, Dieny B, Miranda R and Nogues J 2005 *Phys. Rev. Lett.* **95** 057204